A Theoretical Model for the Orientation of 16-Electron [CpML] Insertion into the C–H Bond of Propane and Cyclopropane and Its Regio- and Stereoselectivity

Ming-Der Su* and San-Yan Chu*[a]

Abstract: Complete geometry optimizations were performed with density functional theory (DFT) in order to study the potential energy surfaces of $[CpM(PH_3)]$ (M = Rh, Ir) complexes inserted into C–H bonds of propane and cyclopropane. The agreement between DFT and experimental results indicates that the B3LYP/LANL2DZ method can be a powerful tool for the investigation of these oxidative addition reactions. A fragment molecular orbital model suggesting the mechanistic pathway for the oxidative addition of saturated alkanes to [CpML] is described. It is shown that these oxidative addition reactions all proceed in a concerted fashion via a three-center transition state, and all lead to exothermic reactions. In particular, we show that both electronic and steric effects play a major role in the preference for a σ_{CH_2}-type of approach, from which one may predict the formation and stabilities of the regio- and stereoselective insertion products. Our theoretical findings suggest that highly reactive $[CpIr(PH_3)]$ tends to be nonless discriminating and reacts randomly, while the less reactive $[CpRh(PH_3)]$ complex is highly selective. We also found that, for both $[CpRh(PH_3)]$ and $[CpIr(PH_3)]$, the ease of oxidative addition is in the order: secondary cyclopropane > primary propane > secondary propane. Furthermore, a configuration mixing model based on the work of Pross and Shaik is used to rationalize the computational results. It is demonstrated that both the singlet–triplet energy gap of 16-electron [CpML] and the $\sigma(C-H) \rightarrow \sigma^*(C-H)$ triplet excitation energy of hydrocarbons play a decisive role in the determination of the reactivity as well as the selectivity of [CpML] insertion.

Keywords: C–H activation · density functional calculations · insertions · oxidative additions

Introduction

Alkanes are unusually stable compounds and they are also among the most abundant organic compounds in nature. Thus, the activation of C–H bonds in saturated hydrocarbons has been a topic of much interest in recent years.[1] Recently, Bergman and co-workers have examined a wide range of alkane substrates with the iridium- and rhodium–$P(CH_3)_3$ complexes. Irradiation of $[\{\eta^5\text{-}C_5(CH_3)_5\}M\{P(CH_3)_3\}H_2]$ in various mixtures of alkane solvents allows the generation of product mixtures which contain alkyl hydrides.[1j, 2] Several general trends can be noted from those observations on the $[\{\eta^5\text{-}C_5(CH_3)_5\}M\{P(CH_3)_3\}]$ systems. Firstly, although the absolute magnitudes of the selectivities are different for iridium and rhodium, their trends are parallel. This observation indicates that C–H oxidative additions proceed by similar mechanisms at these two metal centers, with the rhodium reactions less exothermic than their iridium counterparts. Secondly, there is both a kinetic and thermodynamic preference for the activation of primary C–H bonds over secondary C–H bonds. For the iridium system, the kinetic selectivity is small, while rhodium shows higher kinetic selectivity. Thirdly, there is an inverse correlation of the C–H bond strength and the reactivity of the C–H bond. Namely, the strongest C–H bonds appear to be the most reactive. Fourth, the rhodium system shows a greater thermodynamic selectivity for the less hindered bonds than does iridium. For the former, substrates such as propane or butane show exclusively primary activation products, yet competitive studies of cyclopentane versus benzene or benzene versus propane show that activation of all of the bonds (except the secondary propane bonds) is competitive.

It is these intriguing and important results that aroused our interest. No previous theoretical study has, to our knowledge, been published on the regio- and stereoselectivity in [CpML] reactions.[3] Herein, we therefore chose the system $[CpM(PH_3)] + RH$ [where $(\eta^5\text{-}C_5H_5) = Cp$; M = Rh, Ir; RH = propane, cyclopropane] as a model to study the selectivity of the oxidative addition reactions of an iridium and a rhodium complex to alkane C–H bonds by using density functional theory (DFT). Moreover, the fragment molecular orbital (FMO) and the configuration mixing (CM)

[a] M.-D. Su, Prof. S.-Y. Chu
Department of Chemistry, National Tsing Hua University
Hsinchu 30043, Taiwan (Republic of China)
Fax: (+886) 35-711082
E-mail: ggs§chu1.chem.nthu.edu.tw

0947-6539/99/0501-0198 $ 17.50+.50/0 *Chem. Eur. J.* **1999**, *5*, No. 1

models are used in this work to predict a reaction trajectory for the approach of the [CpML] complex and to develop an explanation for the origin of the barrier height as well as the reaction enthalpy.

Results and Discussion

The electronic structure of the [CpML] + RH model system: We have recently suggested a FMO model,[4] which has been shown to allow the successful prediction of the approximate reaction trajectory and the transition state structure for the insertion of the organometallic fragment into saturated C–H bonds. We shall now apply the FMO model to investigate the oxidative addition reactions of C–H bonds in propane and cyclopropane. We first review briefly the electronic structure of the [CpML] fragment, which has already been analyzed.[5] The frontier orbitals of the 16-electron [CpML] are shown in **1**, in which the highest occupied molecular orbital (HOMO) is a d orbital (a″) that contains a single lone pair of electrons, and the lowest unoccupied molecular orbital (LUMO) is an empty s/p/d hybrid orbital (a′).

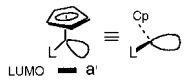

16-electron CpML
1

On the other hand, a localized C–H σ-orbital can be essentially described as having spherical symmetry and [CpML] may approach perpendicularly to the C–H bond axis from any direction (i.e. 360°). This can cause the effect that is very much harder to reconcile with the calculated geometries for the transition state. In fact, in a canonical MO description of a hydrocarbon, there are no isolated MOs that describe a particular C–H σ bond. For example, in methane there is a lower lying $2A_1$ orbital and three degenerate T_2 orbitals.[6] We thus dissect methane into doubly occupied fragment orbitals that have σ-like (σ_{CH_2}, **2**) and π-like (π_{CH_2}, **3**) symmetry.

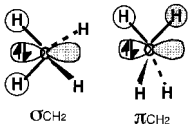

2 **3**

Abstract in Chinese:

本文以密度函數計算方法做完整幾何優選求得 CpM(PH₃)(M=Rh,Ir)插入丙烷暨環丙烷 C-H 鍵的反應位能面。計算結果和實驗符合程度顯示 B3LYP/LANL2DZ 方法是研討氧化加成反應有力工具。使用邊際分子軌域模型分析反應途徑，得知反應涉及三中心協同式的放熱反應，電子暨立體化學效應皆導致σ_{CH_2}反應方位，進而影響生成物選擇性。結果也發現 CpRh(PH₃)較 CpIr(PH₃)有更明顯 C-H 鍵反應選擇性。但二者反應活性順序皆是二級 C-H 鍵(環丙烷) > 一級(丙烷) > 二級(丙烷)。最後我們以 Pross 和 Shaik 的電子組態混合模型的理論來闡明計算結果，可以顯示出 CpML 及碳氫化合物兩者單重態和三重態能量間隔扮演決定反應活化能大小的重要角色。

Since it is easier to visualize the coalescence of the electron donor and acceptor when the approximate axis of the reaction is clearly defined, we therefore prefer to use a canonical MO rather than a localized description of the C–H bond (Figure 1). In this qualitative theoretical treatment, we

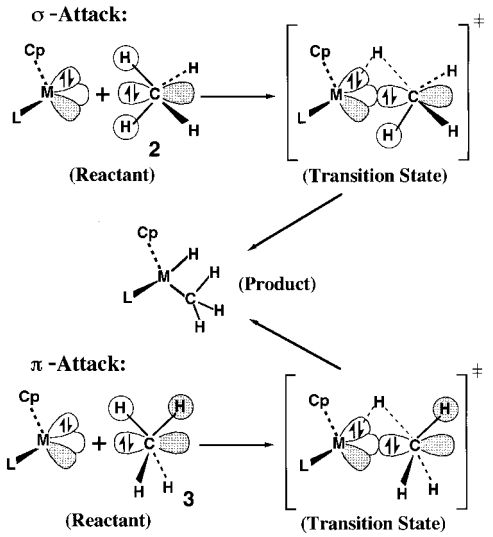

Figure 1. The insertion of [CpML] into hydrocarbons can proceed along a σ_{CH_2} path, where the empty [CpML] s/p/d orbital is aligned with the carbon p orbital of a σ_{CH_2}-fragment orbital, or along a π_{CH_2} path, where the [CpML] s/p/d orbital is aligned with a π_{CH_2}-fragment orbital.

identify the 16-electron fragment [CpML] as having an empty electrophilic orbital (i.e. LUMO in **1**) that could either interact with a filled σ_{CH_2} fragment orbital or approach a π_{CH_2} hydrocarbon orbital. Hence, the implication of a σ_{CH_2} (**2**) or a π_{CH_2} (**3**) fragment orbital in methane identifies a molecular plane that is approached by [CpML] and provides an estimate of the starting geometry in the search for a saddle point. As a result, the net molecular event involved in the insertion of the [CpML] complex into a C–H σ bond of methane is the formation of a new metal–carbon σ bond as well as a new metal–hydrogen σ bond, accompanied by the breaking of the C–H σ bond. This is a typical example for the oxidative addition reaction of a transition metal complex into the C–H bond.[1] It should be pointed out here that this concept of an insertion mechanism was expressed for the first time by Bach et al.[7]

With the above analysis in hand, we would like to extend the methane case to the larger hydrocarbon systems in this work, that is propane and cyclopropane. The requisite canonical MOs for the primary (1°) and secondary (2°) carbon of propane are given in Figure 2. We shall now apply this FMO model depicted in Figure 2 to investigate the mechanism of [CpM(PH$_3$)] insertion.

[CpIr(PH$_3$)] insertion into propane and cyclopropane: The fully optimized geometries of the agostic complex, transition state, and product for the insertion of [CpIr(PH$_3$)] into primary and secondary C–H bonds of propane are given in Figures 3 and 4, respectively.[8] Likewise, in Figure 5 we show the geometrical structures of the stationary points for the

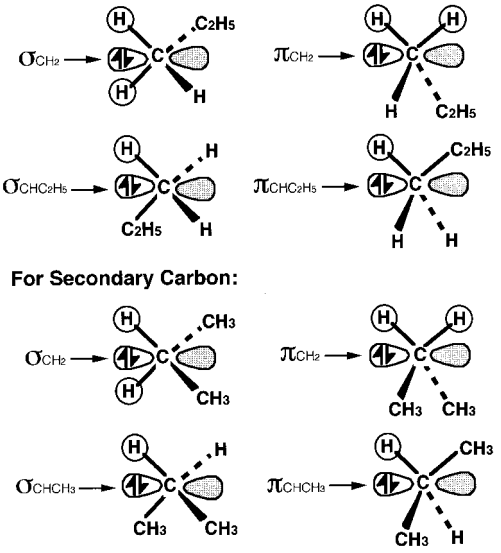

Figure 2. Orientation of [CpML] attack on propane.

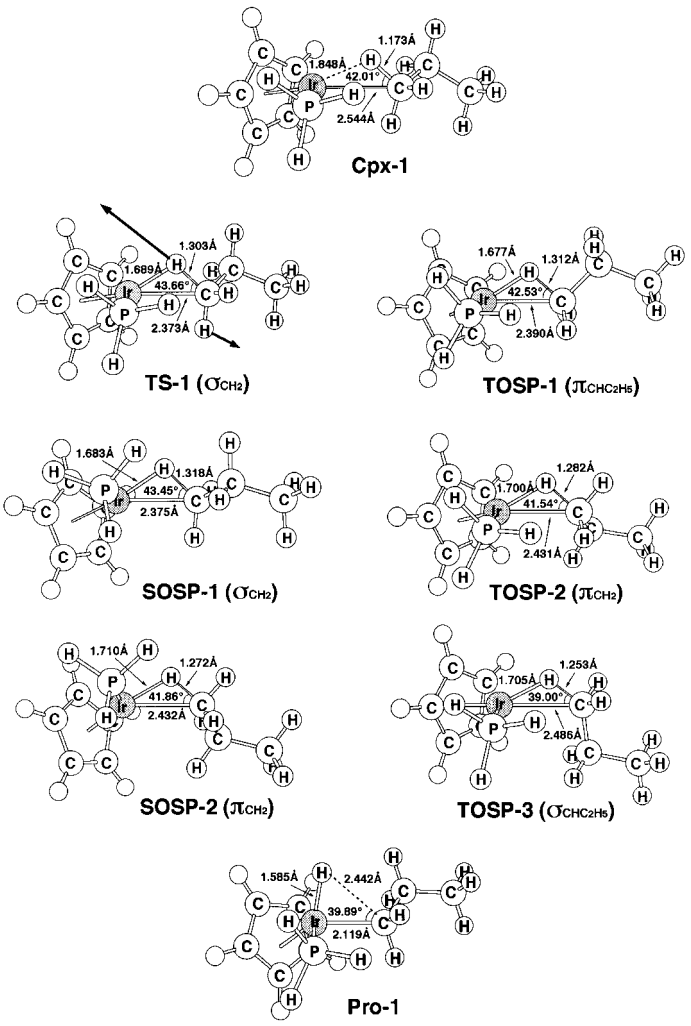

Figure 3. B3LYP/LANL2DZ-optimized geometries of the agostic complex (**Cpx-1**), the transition state (**TS-1**), and the product (**Pro-1**) for [CpIr(PH$_3$)] insertion into the primary C–H bond of propane. The bold arrows indicate the main atomic motions in the transition state eigenvector. SOSP and TOSP represent second-order (two imaginary frequencies) and third-order (three imaginary frequencies) saddle points, respectively.

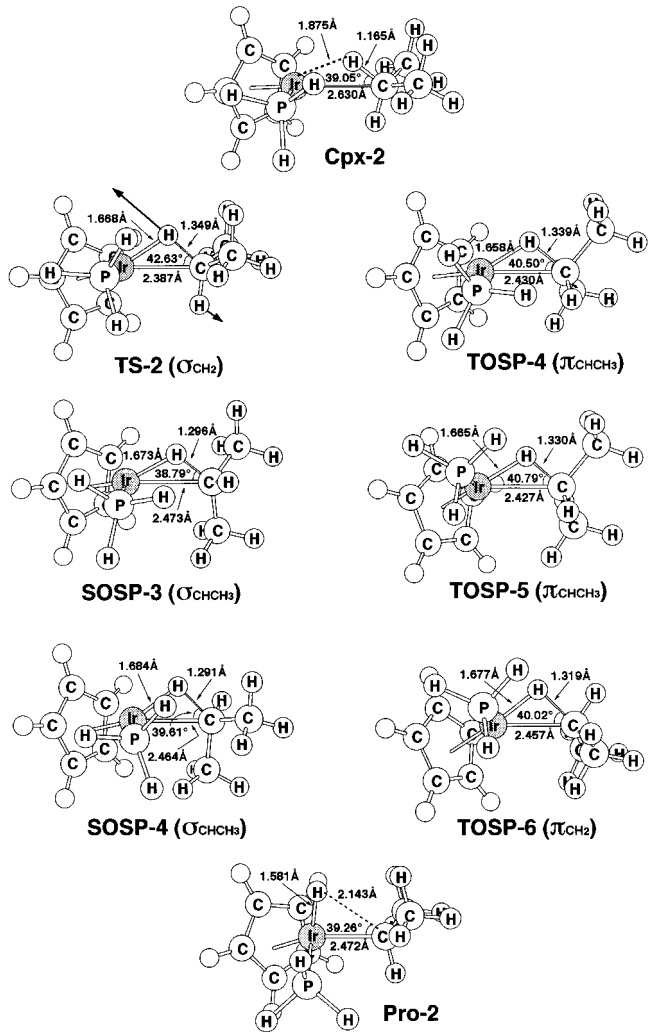

Figure 4. B3LYP/LANL2DZ-optimized geometries of the agostic complex (**Cpx-2**), the transition state (**TS-2**), and the product (**Pro-2**) for [CpIr(PH$_3$)] insertion into the secondary C–H bond of propane. The bold arrows indicate the main atomic motions in the transition state eigenvector. SOSP and TOSP represent second-order (two imaginary frequencies) and third-order (three imaginary frequencies) saddle points, respectively.

oxidative addition of cyclopropane to [CpIr(PH$_3$)]. Their relative energies at the B3LYP/LANL2DZ level are presented in Table 1.

Several interesting results can be drawn from Figures 3–5 and Table 1. Firstly, our DFT calculations suggest that the [CpIr(PH$_3$)] complex in a triplet ground state might insert into the saturated C–H bond by a diradical mechanism. Nevertheless, it is well established that whenever a triplet reactant contains a heavy atom center (such as a transition metal), strong spin-orbit coupling may occur, which can provide a spin-inversion process for transferring to the singlet reactant and then undergoing the singlet reaction.[9] In addition, the results in Table 1 also suggest that the excitation energy from the triplet ground state to the first singlet state for the [CpIr(PH$_3$)] fragment is small (-16.9 kcal mol^{-1}). Both of these considerations should allow the transition from the triplet to the singlet state to occur without difficulty. Indeed, it has been confirmed experimentally that these oxidative additions did not involve any free radicals as

0947-6539/99/0501-0200 $ 17.50+.50/0 *Chem. Eur. J.* **1999**, *5*, No. 1

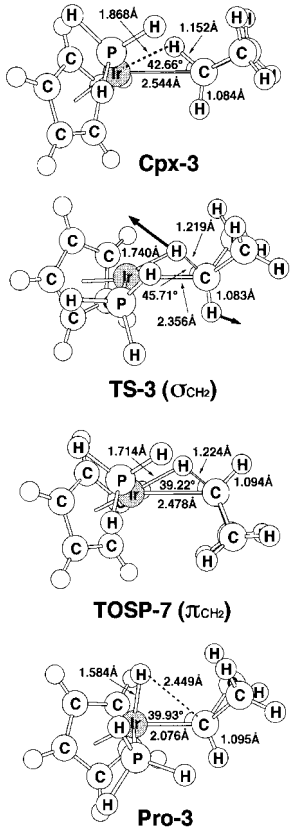

Figure 5. B3LYP/LANL2DZ-optimized geometries of the agostic complex (**Cpx-3**), the transition state (**TS-3**), and the product (**Pro-3**) for [CpIr(PH$_3$)] insertion into the C–H bond of cyclopropane. The bold arrows indicate the main atomic motions in the transition state eigenvector. TOSP represents a third-order (three imaginary frequencies) saddle point.

intermediates.[1b] Thus, it could well be that the oxidative addition reactions proceed on the singlet surface, even if the reactants start from the triplet state. We shall therefore focus on the singlet surface from now on.

Secondly, there are six distinguishable orientations for the insertion of [CpIr(PH$_3$)] into either a primary or a secondary C–H σ bond of propane, while [CpIr(PH$_3$)] may approach cyclopropane from only two unique directions (i.e. σ_{CH_2} and π_{CH_2}). As shown in Figures 3–5, our results strongly indicate that for the approach of [CpIr(PH$_3$)] towards the saturated C–H bonds, a σ-orientated attack is preferred over a π orientation. This can be easily understood by the fact that the [CpIr(PH$_3$)] insertion in a σ_{CH_2} orientation has fewer steric interactions than any other approach and provides the insertion product in its staggered lower energy conformation. As determined by the frequency calculations at the B3LYP/LANL2DZ level, only the σ_{CH_2} approach (**TS-1**, **TS-2**, **TS-3**) can lead to a transition state, whereas the π_{CH_2}, $\sigma_{CHC_2H_5}$, $\pi_{CHC_2H_5}$, σ_{CHCH_3}, and π_{CHCH_3} routes to insertion will yield either second-order saddle points (SOSP, with two imaginary frequencies) or third-order saddle points (TOSP, with three imaginary frequencies). Nevertheless, another σ_{CH_2} transition state for primary insertion of propane, **SOSP-1**, was determined (Figure 3). The B3LYP/LANL2DZ calculation of the frequencies showed that **SOSP-1** has two imaginary frequencies with the second one (85.8*i* cm^{-1}) corresponding to a rotation from the **SOSP-1** towards the **TS-1** conformation; the former is higher in energy than the latter by 1.31 kcal mol^{-1}.

Table 1. Relative energies for the process [CpM(PH$_3$)] + alkane → agostic complex → transition state → product.[a]

Metal	Substrate	Compound	Orientation	Energy
Ir[b]	1° propane	reactants		0
		Cpx-1		−6.56
		TS-1	σ_{CH_2}	−5.78
		SOSP-1	σ_{CH_2}	−4.47
		SOSP-2	π_{CH_2}	−2.39
		TOSP-1	$\pi_{CHC_2H_5}$	−4.31
		TOSP-2	π_{CH_2}	−2.88
		TOSP-3	$\sigma_{CHC_2H_5}$	−1.04
		Pro-1		−34.6
	2° propane	**Cpx-2**		−6.02
		TS-2	σ_{CH_2}	−4.13
		SOSP-3	σ_{CHCH_3}	−0.688
		SOSP-4	σ_{CHCH_3}	−0.377
		TOSP-4	π_{CHCH_3}	−2.01
		TOSP-5	π_{CHCH_3}	−1.32
		TOSP-6	π_{CH_2}	+0.590
		Pro-2		−31.7
	2° cyclopropane	reactants		0
		Cpx-3		−6.07
		TS-3	σ_{CH_2}	−5.77
		TOSP-7	π_{CH_2}	+0.703
		Pro-3		−37.7
Rh[c]	1° propane	reactants		0
		Cpx-4		−10.9
		TS-4	σ_{CH_2}	−1.97
		SOSP-5	σ_{CH_2}	−0.924
		SOSP-6	$\sigma_{CHC_2H_5}$	+1.21
		TOSP-8	$\pi_{CHC_2H_5}$	−0.0481
		TOSP-9	π_{CH_2}	+0.677
		TOSP-10	π_{CH_2}	+0.850
		Pro-4		−15.6
	2° propane	**SOSP-7**	σ_{CH_2}	+0.127
		SOSP-8	σ_{CHCH_3}	+2.61
		SOSP-9	π_{CHCH_3}	+2.64
		SOSP-10	π_{CHCH_3}	+2.85
		SOSP-11	π_{CH_2}	+4.40
		TOSP-11	σ_{CHCH_3}	+2.40
	2° cyclopropane	reactants		0
		Cpx-5		−10.4
		TS-5	σ_{CH_2}	−2.81
		TOSP-12	π_{CH_2}	+2.79
		Pro-5		−17.5

[A] At the B3LYP/LANL2DZ level; in kcal mol^{-1}. [b] The ΔE_{st} of [CpIr(PH$_3$)] is −16.9 kcal mol^{-1}. [c] The ΔE_{st} of [CpRh(PH$_3$)] is −13.2 kcal mol^{-1}.

Thirdly, by examining the single imaginary frequency for each transition state structure, as indicated by the bold arrows in Figures 3–5, it is clear that their transition vectors are all in accordance with the insertion process, primarily the C–H bond stretching with migration of a hydrogen atom to the iridium center. Moreover, as expected,[4] the oxidative addition reaction of [CpIr(PH$_3$)] will include a three-center transition state involving iridium, carbon, and hydrogen atoms. Notably such a characteristic three-center pattern is in accordance with mechanisms postulated by Bergman[10] and Jones.[11]

Fourthly, from the examination of those conformations of the agostic complexes (**Cpx-1**, **Cpx-2**, **Cpx-3**) and the products (**Pro-1**, **Pro-2**, **Pro-3**), as shown in Figures 3–5, it is apparent that the alkane fragment is poised in a σ_{CH_2} fashion, which is

consistent with the above findings for the transition state in which the σ_{CH_2} orientation is favored over other approaches. Thus, the reaction trajectory for C–H insertion suggested by this FMO model appears to be applicable in both the agostic complex and the product.

Fifthly, the activation barrier from the precursor complex to the transition state at the B3LYP/LANL2DZ level increases in the order (Table 1): 2° cyclopropane (0.306 kcal mol^{-1}) < 1° propane (0.786 kcal mol^{-1}) < 2° propane (1.89 kcal mol^{-1}). Likewise, their order of exothermicity follows the same trend as the activation energy: 2° cyclopropane (−37.7 kcal mol^{-1}) < 1° propane (−34.6 kcal mol^{-1}) < 2° propane (−31.7 kcal mol^{-1}). Our computational results provide strong evidence that the ease of oxidative addition is in the order 2° cyclopropane > 1° propane > 2° propane, which is in good agreement with the experimental trends.[2a] It is noteworthy that the secondary insertion of cyclopropane is highly preferred compared to that of propane, even though the former only contains secondary carbon centers (vide infra).

Sixthly, we next examined the preferred orientation of the breaking C–H bond with respect to the [CpML] lone pair (HOMO in **1**). Intuitively, hydrogen migration to the larger lobe of the HOMO of [CpML] should have a lower activation barrier since this can result in a good overlap between the migrating hydrogen and the central metal and would stabilize the transition state. Thus, the stabilization energy of the transition state should depend upon the M–C bond length and the M-C-H bond angle (C–H represents the breaking C–H bond). In other words, both the smaller M–C distance and the larger M-C-H angle should enhance the activation of alkane C–H bonds by [CpML]. As shown in Figures 3–5, the Ir–C distance increases in the order 2° cyclopropane (2.36 Å, **TS-3**) < 1° propane (2.37 Å, **TS-1**) < 2° propane (2.39 Å, **TS-2**), while the Ir-C-H angle decreases in the order 2° cyclopropane (45.7°, **TS-3**) > 1° propane (43.7°, **TS-1**) > 2° propane (42.6°, **TS-2**). This structural evidence is again consistent with the above prediction. We shall discuss the origin of barrier heights in more detail after consideration of the Rh case.

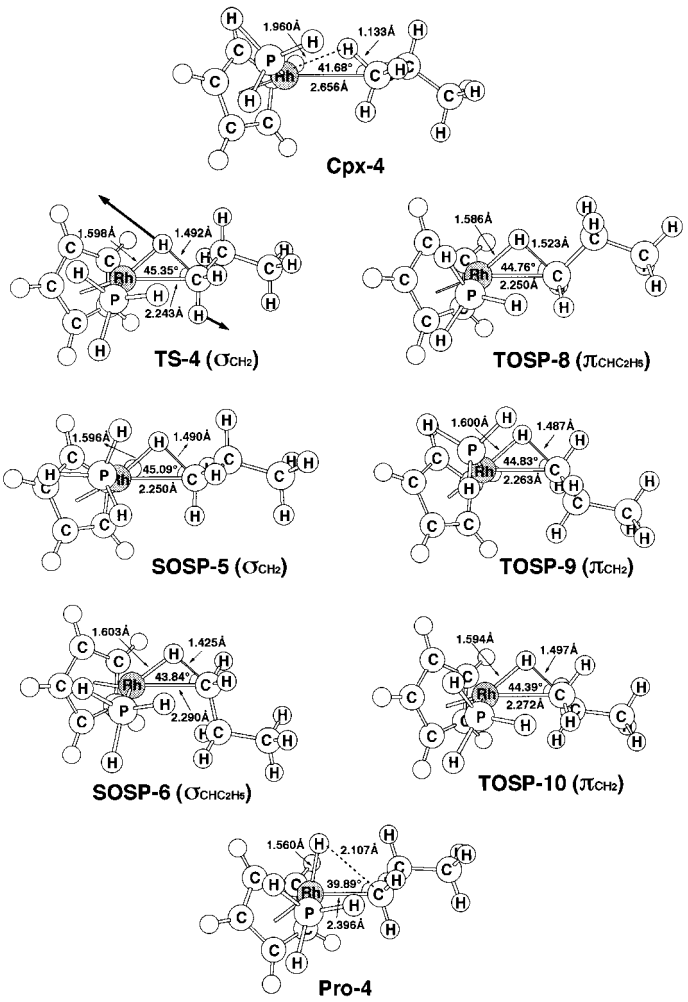

Figure 6. B3LYP/LANL2DZ-optimized geometries of the agostic complex (**Cpx-4**), the transition state (**TS-4**), and the product (**Pro-4**) for [CpRh(PH$_3$)] insertion into the primary C–H bond of propane. The bold arrows indicate the main atomic motions in the transition state eigenvector. SOSP and TOSP represent second-order (two imaginary frequencies) and third-order (three imaginary frequencies) saddle points, respectively.

[CpRh(PH$_3$)] insertion into propane and cyclopropane: The fully optimized geometries of the agostic complex, transition state, and product for the insertion of [CpRh(PH$_3$)] into primary and secondary C–H bonds of propane and cyclopropane are shown in Figures 6–8, respectively.[8] Their relative energies at the B3LYP/LANL2DZ level are presented in Table 1.

Three points are noteworthy: Firstly, the computational results of the reaction with [CpRh(PH$_3$)] are, in principle, similar to those noted above for the [CpIr(PH$_3$)] system in many aspects. For instance, our theoretical investigations suggest that the σ_{CH_2} orientation for [CpRh(PH$_3$)] insertion into saturated C–H bonds will be preferred to other approaches which will lead to high-order saddle points, a characteristic three-center pattern for the transition state, and hydrogen migration to the larger lobe of HOMO of the attacking [CpRh(PH$_3$)]. In addition, as shown in Table 1, DFT calculations predict that the insertion of [CpRh(PH$_3$)], from the agostic complex through the transition state to the product, is thermodynamically exothermic by −17.5 kcal mol^{-1} (2° cyclopropane) and −15.6 kcal mol^{-1} (1° propane) with an activation energy of 7.57 kcal mol^{-1} (2° cyclopropane) and 8.96 kcal mol^{-1} (1° propane), respectively, from the agostic complex. Again, our results strongly indicate that the secondary insertion of cyclopropane is more favorable than the primary insertion of propane (vide infra).

Secondly, according to the B3LYP/LANL2DZ results, it is interesting to point out that the transition state for secondary insertion of propane has never been found (see Figure 7). Of the six possible routes for secondary C–H activation, the most promising one is **SOSP-7** (σ_{CH_2}-attack), which has the lowest energy compared to the other five approaches. Calculations of the energy Hessian revealed two imaginary frequencies for **SOSP-7**: that at $\tilde{\nu} = 906i$ cm^{-1} is a vibrational mode corresponding to the reaction coordinate insertion into the secondary C–H bond of propane, the other at $\tilde{\nu} = 78.7i$ cm^{-1} is, however, a major rotation of the *sec*-propyl fragment. A distortion along the second imaginary mode was attempted and was followed by a geometry optimization without any symmetry constraints. This led directly to

0947-6539/99/0501-0202 $ 17.50+.50/0 *Chem. Eur. J.* **1999**, *5*, No. 1

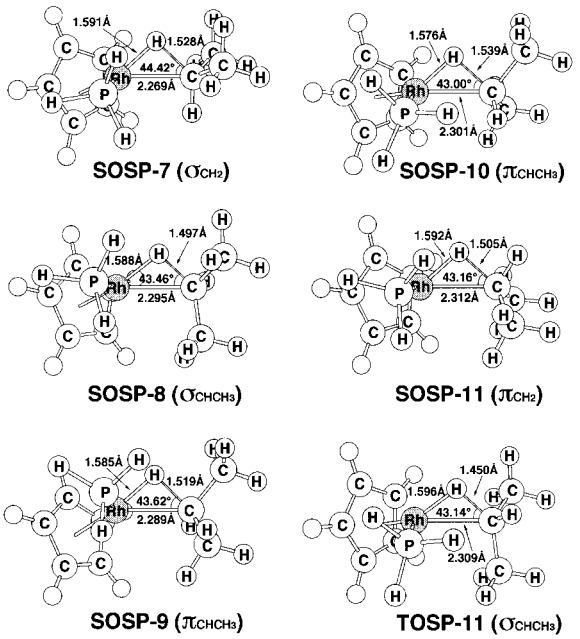

Figure 7. B3LYP/LANL2DZ-optimized geometries of the transition state for [CpRh(PH_3)] insertion into the secondary C–H bond of propane. TOSP represents a third-order (three imaginary frequencies) saddle point. See the text.

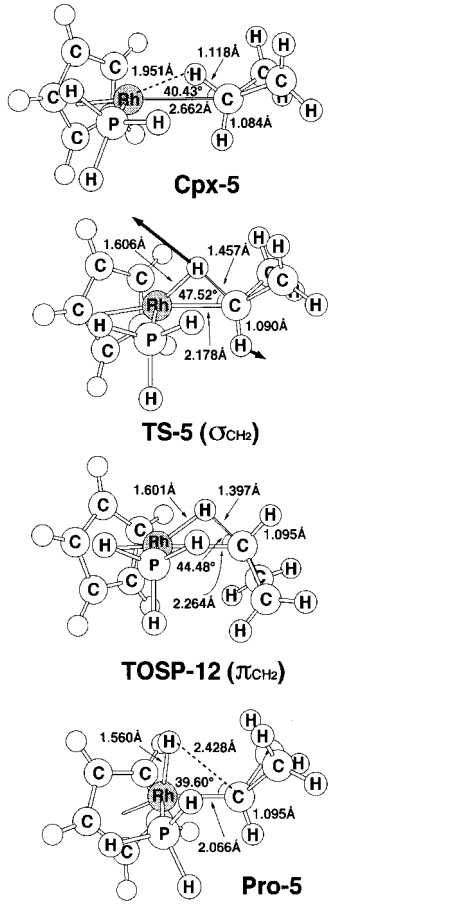

Figure 8. B3LYP/LANL2DZ-optimized geometries of the agostic complex (**Cpx-5**), the transition state (**TS-5**), and the product (**Pro-5**) for [CpRh(PH_3)] insertion into the C–H bond of cyclopropane. The bold arrows indicate the main atomic motions in the transition state eigenvector. TOSP represents a third-order (three imaginary frequencies) saddle point.

TOSP-11 (σ_{CHCH_3}) with three imaginary frequencies. The reduction of the optimization convergence criteria by an order of magnitude still did not alter the situation. Moreover, attempts to find any transition state for secondary insertion of propane were unsuccessful. It seems likely that the potential energy surface for [CpRh(PH_3)] insertion into secondary propane is fairly flat and the problem is simply one of insufficient numerical accuracy in Hessian.[12] Nevertheless, the secondary insertion product of cyclopropane can be detected experimentally.[2] Our theoretical investigations support this experimental observation. As shown in Figure 8, we obtained its transition state (**TS-5**) with a single imaginary frequency ($\tilde{\nu} = 836i\ cm^{-1}$). Animation of this imaginary frequency clearly shows a rocking motion of the entire σ_{CH_2} fragment, as indicated by the bold arrows. Consequently, in contrast to [CpIr(PH_3)] insertion, [CpRh(PH_3)] insertion should result in the following trend: 2° cyclopropane > 1° propane >> 2° propane. In other words, the rhodium complex is significantly more discriminating than the iridium complex. This has been confirmed experimentally,[2] as mentioned in the Introduction.

Thirdly, the energy of the transition state for cyclopropane insertion is below that of its corresponding reactants ([CpRh(PH_3)] + cyclopropane) (Table 1). This indicates that the rearrangement shown in **4** can occur without the

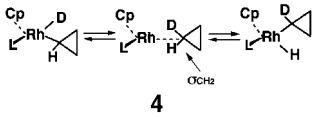

4

dissociation of cyclopropane from the [CpRh(PH_3)] fragment. Consequently, the agostic complex we found in this work may correspond to the intermediate η^2 complex proposed by Periana and Bergman for α migration.[2b] Moreover, as shown in Figure 8, our DFT calculations suggest that the Rh agostic complex (**Cpx-5**) should be a structure in which cyclopropane is bound in an end-on fashion through two hydrogen atoms, that is in a σ_{CH_2} fashion, which is again in accordance with the mechanism postulated by Periana and Bergman.[2b] For these reasons, our theoretical results provide strong support for the existence of alkane η^2-complex intermediates, which intervene in the oxidative addition process to saturated hydrocarbons before full C–H bond cleavage occurs.

Before further discussion, we shall summarize the resulting potential energy profiles at the B3LYP/LANL2DZ level in Figure 9. From the above discussion and Figure 9, we thus obtained the following conclusions, all of which have been confirmed by experimental findings:[1j, 2]

1) The reaction of [CpML] with propane and cyclopropane must be competitive, since the energy difference between them is small. Additionally, the order of reactivity of C–H bonds toward [CpML] attack is 2° cyclopropane > 1° propane > 2° propane.
2) The oxidative addition of the iridium complex is preferred both kinetically and thermodynamically over that of the rhodium complex. In addition, the rhodium insertion is much more selective than the iridium insertion.

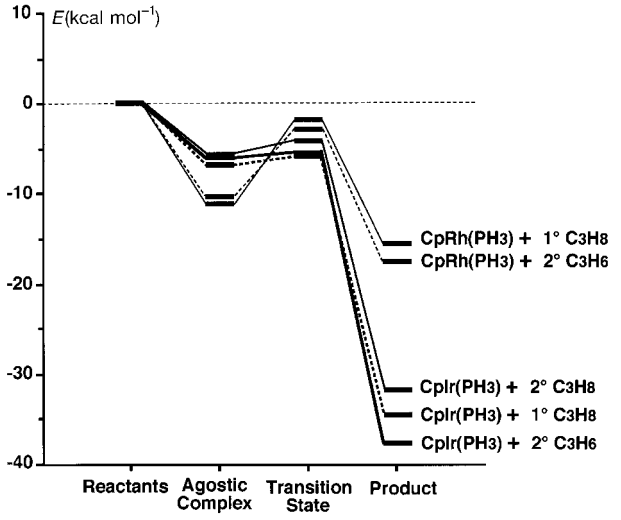

Figure 9. Potential energy surfaces for the activation of propane and cyclopropane C–H bond by [CpM(PH_3)] (M = Rh, Ir). The relative energies are taken from the B3LYP/LANL2DZ values given in Table 1. For the B3LYP-optimized structures of the stationary points see Figures 3–8.

3) The 16-electron [CpML] fragment will preferentially approach a saturated hydrocarbon in a concerted σ_{CH_2} fashion.
4) Due to some additional steric repulsions caused by the effect of alkyl substitution, the tertiary hydrocarbons fail to react with [CpML].

One may therefore apply the above conclusions to predict the potential existence of regio- and stereoselective products in oxidative addition of hydrocarbon C–H bonds to [CpML]. For instance, inspection of cyclohexane (**5**) suggests that a π_{CH_2} approach across the top of the six-membered ring would be sterically hindered by the axial hydrogens. Moreover, we predict that the 16-electron [CpML] complex would approach cyclohexane in a σ_{CH_2} fashion as expected in point 3). In other words, both electronic and steric effects play a decisive role in the preference for a σ_{CH_2} approach.

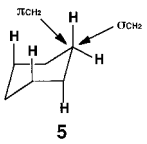

5

The configuration mixing model: Recently, it has been shown that the configuration mixing (CM) model, based on the work of Pross and Shaik,[13] can be used to understand the origin of barrier heights for carbene insertion reactions.[14] Since 16-electron [CpML] is known to be isolobal to CH_2,[15] it is, in principle, conceivable that, with the use of the isolobal analogy, the same predictions could also be applied to organometallic systems.[4b] We would like to use this model to gain a better understanding of the reactivity of the various C–H bonds in propane with respect to cyclopropane as well as the selectivity of the 16-electron [CpML] (M = Rh, Ir) complexes.

In the CM model the total energy profile is broken down into two component curves: the one associated with the reactant bonding situation, is denoted as the *reactant configuration* and the other, associated with the product bonding situation, is denoted as the *product configuration*. The crossing of the two curves detects the transition state and the energy barrier.

In Figure 10, we represent the qualitative behavior of the two configurations for the [CpML] oxidative addition to an alkane C–H bond. The reactant configuration describes a situation in which the two electrons on the [CpML] fragment

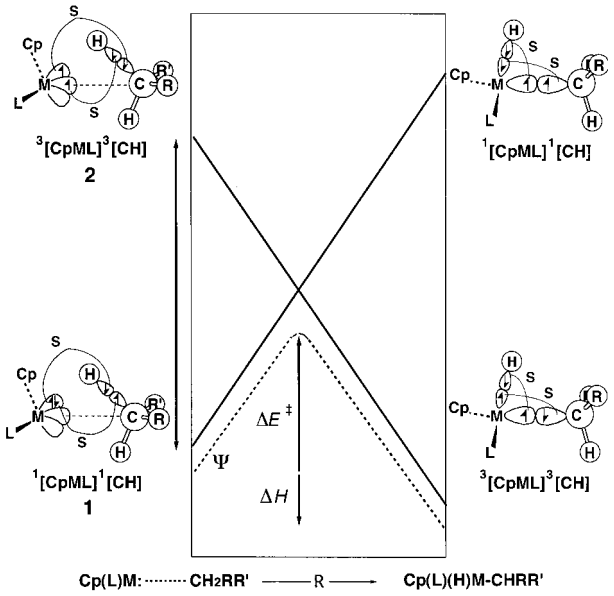

Figure 10. Energy diagram for an oxidative addition reaction showing the formation of a state curve (Ψ) on mixing two configurations: the reactant configuration and the product configuration. It is apparent that both the activation energy ($\Delta E^{\ddagger}$) and reaction enthalpy (ΔH) is proportional to ΔE_{st} ($= E_{triplet} - E_{singlet}$ for 16-electron [CpML]) and $\Delta E_{\sigma\sigma^*}$ ($= E_{triplet} - E_{singlet}$ for the alkane). S represents a singlet. See the text.

are spin-paired to form the lone pair, while the two electrons on the alkane moiety are spin-paired to form a C–H σ bond. Its valence bond (VB) configuration is labeled ^{1}[CpML]^1[CH] (**6**). On the other hand, the product configuration corresponds to a situation in which the electron pairs are coupled to allow both M–H and M–C bond formation and simultaneous C–H bond breaking. Note that the spin arrangement is now different, as seen in its VB product configuration (**7**). In order to obtain this configuration from the reactant configuration **6**, each of the two original electron pairs needs to be uncoupled, which requires the excitation of the electron pairs from the singlet state to the triplet state. Hence, this configuration is labeled ^{3}[CpML]^3[CH]. Notably ^{3}[CpML]^3[CH] is an overall singlet configuration, despite the fact that it contains two local triplets. The MO representations of VB configurations **6** and **7** are shown in **8** and **9**,

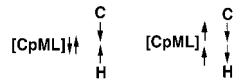

6 **7**

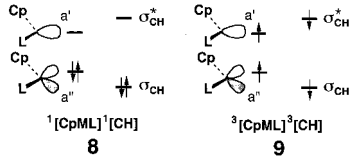

8 **9**

0947-6539/99/0501-0204 $ 17.50+.50/0 *Chem. Eur. J.* **1999**, *5*, No. 1

respectively. As mentioned above, it is the avoided crossing of these two configurations that leads to the simplest description of the ground state energy profiles for oxidative addition reactions of 16-electron [CpML] complexes.

As shown in Figure 10, it is apparent that the barrier height ($\Delta E^{\neq}$) as well as the reaction enthalpy (ΔH) may be expressed in terms of the initial energy gap between the reactant and product configurations. In other words, this model shows that the existence of the barrier is due to the combined effect of two factors: the singlet–triplet energy gap of [CpML] ($\Delta E_{st} = E_{triplet} - E_{singlet}$ for 16-electron [CpML]) and the $\sigma(C-H) \rightarrow \sigma^*(C-H)$ triplet excitation energy of the alkane ($\Delta E_{\sigma\sigma^*} = E_{triplet} - E_{singlet}$ for alkane). Accordingly, supposing $\Delta E_{\sigma\sigma^*}$ is a constant, a smaller value of ΔE_{st} would lead to: i) reduction of the reaction barrier since the intended crossing of ^{1}[CpML]^1[CH] and ^{3}[CpML]^3[CH] is lower in energy, and ii) a larger exothermicity since the energy of the product is now lower than that of the reactant. Likewise, if ΔE_{st} of [CpML] is a constant, then a smaller value of $\Delta E_{\sigma\sigma^*}$ would also lead to a lower barrier height and a larger exothermicity. Bearing this CM model (Figure 10) in mind, we shall explain the origin of the observed trends as shown previously in the following discussion:

Why is the Ir reaction more favorable than the Rh reaction in the activation of the C–H bond? The reason for this can be traced to the singlet–triplet energy gap (ΔE_{st}) of [CpML]. As analyzed above, the smaller the value of ΔE_{st} of [CpML] (if $\Delta E_{\sigma\sigma^*}$ is a constant), the lower the barrier height and the larger the exothermicity, and, in turn, the faster the oxidative addition reaction. Furthermore, as Siegbahn has pointed out,[16] the Ir atom has a quartet d^7s^2 ground state with a high excitation energy to the doublet d^9 state (61 kcal mol^{-1}). The Rh atom has a quartet d^8s^1 ground state but with a relatively low excitation energy to the doublet d^9 state (7.8 kcal mol^{-1}). This implies that Ir would prefer to remain in a high-spin state, whereas Rh favors a low-spin state. It is reasonable to expect that the promotion energy from the singlet state to the triplet state, used to form the strongest covalent bonds, should be smaller for the Ir complex than for the Rh complex. Our B3LYP/LANL2DZ results suggest that ΔE_{st} of [CpIr(PH$_3$)] (-16.9 kcal mol^{-1}) is smaller in energy than that of [CpRh(PH$_3$)] (-13.2 kcal mol^{-1}), which is consistent with the above prediction. For this reason, insertion into a C–H bond is more facile and more exothermic for the Ir system than for its Rh counterpart.

Why does the reactivity of C–H bonds decrease in the order: 2° cyclopropane > 1° propane > 2° propane? The driving force of this may be traced to $\Delta E_{\sigma\sigma^*}$, which can be evaluated to a good approximation from the energies of the vertical $\sigma(C-H) \rightarrow \sigma^*(C-H)$ triplet excitation in alkane. As anticipated by the CM model, if ΔE_{st} of [CpML] is a constant, then a smaller value of $\Delta E_{\sigma\sigma^*}$ leads to a lower barrier height and a larger exothermicity. Our DFT results suggest an increasing trend in $\Delta E_{\sigma\sigma^*}$ for 2° cyclopropane (206 kcal mol^{-1}) < 1° propane (254 kcal mol^{-1}) < 2° propane (259 kcal mol^{-1}),[17a] in accordance with the trend of the activation energy as well as the enthalpy ($\Delta E^{\neq}$, ΔH) for [CpIr(PH$_3$)] insertion which are (0.306, -37.7), (0.786, -34.6), (1.89, -31.7) kcal mol^{-1},[17b] respectively (Table 1). Note that the ordering of the C–H bond strength follows a different trend than $\Delta E_{\sigma\sigma^*}$: cyclopropane ($106.3 \pm 0.3$ kcal mol^{-1})[18] > 1° propane (100.4 ± 0.6 kcal mol^{-1})[19] > 2° propane (98.6 ± 0.4 kcal mol^{-1})[20] (vide infra).

The comparison between the propane and cyclopropane reactions provides additional insight into the dominating electronic effects in the oxidative addition of unsaturated C–H bonds. One mystifying and surprising result that has emerged from the active research on the C–H oxidative addition reaction is that there is a general *inverse* correlation between the initial C–H bond strength and the ease of activation of this bond by transition metal complexes. This is exactly opposite to what might have been predicted based upon C–H bond breaking alone.[1e,g, 21] For instance, despite the fact that the C–H bond strengths in methane, ethylene, and acetylene are 104.8 ± 0.4,[22] 111.2 ± 0.8,[23] and 132.9 ± 0.7 [23, 24] kcal mol^{-1}, respectively, it has been shown that the methane C–H bond is more difficult to activate than the ethylene C–H bond, which in turn is more difficult to activate than the acetylene C–H bond.[21] The simplest explanation of the origin of the differences in activation barriers is a steric effect. As Siegbahn and Blomberg have pointed out,[21] since C–H activation requires that the central metal efficiently interacts in a sideways orientation to the C–H bond, it is clear that this position is most easily reached for acetylene. For methane, however, a substantial initial distortion of the molecule is needed to reach a proper interaction. For ethylene, the situation is somewhere in between that of acetylene and methane. In other words, even though the data is only qualitative at this point, it is apparent that the C–H bond with sp character is strongly favored, sp^2 is the next easiest, and sp^3 is the most difficult. The C–H acidities, rather than bond energies, control the rate of attack of the metal center on particular C–H bonds.

According to this study, it is shown that the CM model emphasized here may supplement the above results. Namely, an understanding of singlet–triplet splitting $\Delta E_{\sigma\sigma^*}$ is crucial for the prediction of the reactivity of different C–H bonds of hydrocarbons. For example, our B3LYP/LANL2DZ calculations indicate that the values of $\Delta E_{\sigma\sigma^*}$ for different C–H bonds are in the order acetylene (101 kcal mol^{-1}) < ethylene (147 kcal mol^{-1}) < methane (291 kcal mol^{-1}),[17] which follows the same trend as the ease of the C–H bond breaking as mentioned above. Though we have not carried out these calculations for different C–H bond activations by transition metal complexes with the same level of theory in this work, the fact that the above $\Delta E_{\sigma\sigma^*}$ trend agrees reasonably well with the order of insertion activity reported experimentally[1e,g, 25] and theoretically[21] shows that, besides the steric effect, the electronic effect must also play a role in oxidative addition of hydrocarbon C–H bonds.

Why is the Rh complex much more selective than the iridium counterpart in oxidative addition of C–H bonds? In fact, chemical reactivity and selectivity are generally thought to be inversely related to each other.[13b, 26] More specifically, in a

series of related reactions the more reactive reagents will exhibit smaller selectivity and, conversely, that the less reactive reagents will exhibit greater selectivity. This pattern of behavior has been generalized into what is termed as the *reactivity–selectivity principle*.[13b, 26] In oxidative addition reactions, the highly reactive [CpIr(PH_3)] complex was found to be less discriminate in its reaction with different C–H bonds of the same molecule than the less reactive [CpRh(PH_3)], as illustrated in Figure 9. This can be derived from the Marcus theory.[27] It has been shown that, based on a two-curve avoided-crossing model (i.e., CM model, Figure 10), an inverse relationship between reactivity and selectivity is anticipated.[13b] Namely, it is the ΔE_{st} and $\Delta E_{\sigma\sigma^*}$ factors that govern reactivity as well as the selectivity of the 16-electron [CpML] complexes. When ΔE_{st} (or $\Delta E_{\sigma\sigma^*}$) is small, the activation barrier is small, and the transition state resembles the reactants; thus reactivity is high and selectivity is small. On the contrary, when ΔE_{st} (or $\Delta E_{\sigma\sigma^*}$) is large, the barrier height is large and the transition state resembles the product; so reactivity is small and selectivity is high. For instance, since it has already been shown that ΔE_{st} of [CpRh(PH_3)] is larger than that of [CpIr(PH_3)] and $\Delta E_{\sigma\sigma^*}$ of 2° propane is also larger than those of 1° propane and 2° cyclopropane, it is perhaps not surprising that [CpRh(PH_3)] is hard to insert into the secondary C–H bond of propane. Thus, in the rhodium series, only primary products are formed from acyclic alkanes. Moreover, according to a Marcus description of reactivity, reactive systems with early transition states are predicted to be less selective than unreactive ones with late transition states.[13b, 27] The comparison of geometries of the transition states (**TS-1**, **TS-2**, **TS-3**) with those of the products (**Pro-1**, **Pro-2**, **Pro-3**) on one side and of the agostic complexes (**Cpx-1**, **Cpx-2**, **Cpx-3**) on the other side, (Figures 3–5), shows that the highly reactive [CpIr(PH_3)] complex reaches the transition state relatively early (reactant-like). In contrast to Ir insertion, comparison of the geometrical parameters among the stationary points in [CpRh(PH_3)] model systems (Figures 6–8) shows that transition states (**TS-4**, **TS-5**) are closer to their corresponding products (**Pro-4**, **Pro-5**) than to agostic complexes (**Cpx-4**, **Cpx-5**), respectively, indicating that the less reactive [CpRh(PH_3)] complex arrives at the transition state relatively late (product-like). Again, our theoretical findings are in qualitative agreement with Marcus theory.

Conclusions

We have studied the reaction mechanisms of the insertion of the 16-electron [CpM(PH_3)] (M = Rh, Ir) fragment into the C–H bond of propane and cyclopropane by density functional theory. Our model calculations have shown that the B3LYP/LANL2DZ level of theory is appropriate to investigate transition-metal insertion processes since it can reproduce the experimental trends correctly. Moreover, this work has represented an attempt to apply the FMO model to predict the approximate reaction trajectory and transition state structures for insertion reactions. Also, we have demonstrated that the computational results can be rationalized by the use of a simple CM model. Thus, not only have we given explanations of the experimental results for those oxidative addition reactions, but we have also made predictions of the potential existence of regio- and stereoselective products. Our study has shown that the problems concerning reactivity as well as selectivity of the 16-electron [CpML] systems can be reduced to pictorial considerations. In spite of its simplicity, our approaches prove to be quite effective and can provide chemists with mechanistic insights into the factors controlling the activation of hydrocarbon C–H bonds, thus allowing a better understanding of the nature of such systems as well as a number of predictions to be made. It is hoped that our study will provide stimulation for further research into the subject.

Methods of Calculation

All geometries were fully optimized without imposing any symmetry constraints. For our DFT calculations, we used the hybrid gradient-corrected exchange functional proposed by Becke,[28a,b] combined with the gradient-corrected correlation functional of Lee, Yang, and Parr.[28c] This functional is commonly known as B3LYP, and has been shown to be quite reliable for geometries.[17, 29]

Effective core potentials (ECPs) were used to represent the 28 innermost electrons of rhodium (up to the 3d shell).[30] Likewise, ECPs were used to represent the 60 innermost electrons of the iridium (up to the 4f shell) atom.[30] For phosphorus we also used the Hay and Wadt relativistic ECP.[31] For these atoms, the basis set was that associated with the pseudopotential, with a standard LANL2DZ contraction.[32] For hydrogen and carbon atoms the double zeta basis of Dunning–Huzinaga was used.[33] We denote our B3LYP calculations by B3LYP/LANL2DZ. Thus, the model compounds [CpM(PH_3)]·C_3H_8 and [CpM(PH_3)]·C_3H_6 (M = Ir, Rh) have 134 (86 electrons) and 130 (84 electrons) basis functions, respectively.

Vibrational frequencies at stationary points were calculated at the B3LYP/LANL2DZ level of theory to identify them as minima (zero imaginary frequencies) or transition states (one imaginary frequency), or higher order saddle points (two or three imaginary frequencies). All calculations were performed with the GAUSSIAN 94/DFT package.[32]

How does one obtain the $\Delta E_{\sigma\sigma^*}$ energy for the C–H bonds in the hydrocarbons? For instance, consider the ethylene case. Its bonding π(C=C) and σ(C–H) molecular orbitals together with the antibonding π*(C=C) and σ*(C–H) molecular orbitals are shown in Scheme 1. It is clearly seen that the HOMO (π) and LUMO (π*) are localized on the carbon atoms; both of them have no electron density associated with the C–H groups. On the other hand, the σ(C–H) and σ*(C–H) molecular orbitals are localized on the four C–H groups. Consequently, $\Delta E_{\sigma\sigma^*}$ can be easily obtained by evaluating the energies of the vertical σ(C–H) → σ*(C–H) triplet excitation. The same situation can also be applied to CH_4 and acetylene molecules.

How does one obtain the $\Delta E_{\sigma\sigma^*}$ energy for the primary and secondary C–H bonds in propane and cyclopropane? For simplicity, we use the orbital contour pictures to explain how to obtain the value of $\Delta E_{\sigma\sigma^*}$. The orbital contour pictures are based on those from reference [6a], p. 165–166 (for propane) and p. 153–155 (for cyclopropane).

As seen in p. 165–166 of reference [6a], in propane (C_{2v} symmetry) the HOMO ($4B_2$) is not only largely associated with the bonding between carbon atoms, but also has a low electron density associated with the terminal 1° CH_3 group. It has to be emphasized that no electron density at all is associated with the central 2° CH_2 group since it is on the nodal plane. Thus, we also call this orbital σ(1° C–H). In contrast, the next two

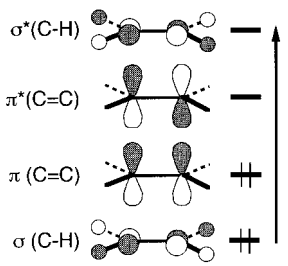

Scheme 1. The bonding and antibonding molecular orbitals of ethylene.

0947-6539/99/0501-0206 $ 17.50+.50/0 *Chem. Eur. J.* **1999**, *5*, No. 1

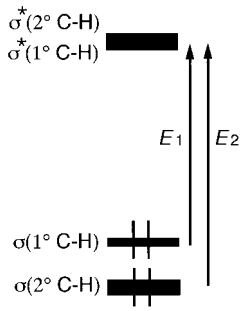

Scheme 2. The vertical σ(C–H) →σ*(C–H) triplet excitation of the C–H bonds in propane.

orbitals ($2B_1$ and $1A_2$) in propane are almost degenerate and their greatest electron density is associated with the hydrogen atoms attached to the central carbon atom. So we call them σ(2° C–H). The same situation can also be found in the unoccupied antibonding orbitals. That is, the LUMO has two almost degenerate orbitals ($3B_1$ and $7A_1$) and their electron density delocalizes on both 1° CH_3 and 2° CH_2 groups. Thus, we can call them σ*(1° C–H) and σ*(2° C–H), respectively. As such, in order to obtain the $\Delta E_{\sigma\sigma^*}$ energies for the C–H bonds in propane, we can evaluate the energies of the vertical σ(C–H) →σ*(C–H) triplet excitation. As shown in Scheme 2, there will be two excitation energies for $\Delta E_{\sigma\sigma^*}$. One is E_1, which is σ(1° C–H) →σ*(1° C–H) for the primary C–H bond. The other is E_2, which is σ(2° C–H) →σ*(2° C–H) for the secondary C–H bond. The same situation can also be applied to cyclopropane. These phenomena can surely be found in the orbitals of the current methodology.

Acknowledgments

We would like to thank the National Center for High-Performance Computing of Taiwan and the Computing Center at Tsing Hua University for generous amounts of computing time, and the National Science Council of Taiwan for their financial support. We wish to thank Professor H. B. Schlegel for providing useful software. We are also grateful to referees for their critical comments and helpful corrections to the manuscript.

[1] For reviews see: a) G. W. Parshall, *Acc. Chem. Res.* **1975**, 8, 113; b) R. G. Bergman, *Science* **1984**, 223, 902; c) A. H. Janowicz, R. A. Perima, J. M. Buchanan, C. A. Kovac, J. M. Struker, M. J. Wax, R. G. Bergman, *Pure Appl. Chem.* **1984**, 56, 13; d) C. L. Hill, *Activation and Functionalization of Alkanes*, Wiley, New York, **1989**; e) J. Halpern, *Inorg. Chim. Acta* **1985**, 100, 41; f) M. Ephritikhine, *New J. Chem.* **1986**, 10, 9; g) W. D. Jones, F. J. Feher, *Acc. Chem. Res.* **1989**, 22, 91; h) A. D. Ryabov, *Chem. Rev.* **1990**, 90, 403; i) J. A. Davies, P. L. Watson, J. F. Liebman, A. Greenberg, *Selective Hydrocarbon Activation, Principles and Progress*, VCH, New York, **1990**; j) R. G. Bergman, *Adv. Chem. Series* **1992**, 230, 211; k) R. H. Crabtree, *Angew. Chem.* **1993**, 105, *828; Angew. Chem. Int. Ed. Engl.* **1993**, 32, 789; l) B. A. Amdtsen, R. G. Bergman, T. A. Mobley, T. H. Peterson, *Acc. Chem. Res.* **1995**, 28, 154.

[2] a) R. A. Periana, R. G. Bergman, *Organometallics* **1984**, 3, 508; b) R. A. Periana, R. G. Bergman, *J. Am. Chem. Soc.* **1986**, 108, 7332; c) ref. [1d], Chapt. 6.

[3] Several theoretical studies have been aimed at examining the chemistry of methane C–H bonds with a 16-electron [CpML] complex, see: a) T. Ziegler, V. Tschinke, L. Fan, A. D. Becke, *J. Am. Chem. Soc.* **1989**, 111, 9177; b) J. Song, M. B. Hall, *Organometallics* **1993**, 12, 3118; c) D. G. Musaev, K. Morokuma, *J. Am. Chem. Soc.* **1995**, 117, 799; d) P. E. M. Siegbahn, *J. Am. Chem. Soc.* **1996**, 118, 1487; e) R. Jimenez-Catano, M. B. Hall, *Organometallics* **1996**, 15, 1889.

[4] a) M.-D. Su, S.-Y. Chu, *Organometallics* **1997**, 16, 1621; b) M.-D. Su, S.-Y. Chu, *J. Am. Chem. Soc.* **1997**, 119, 5373; c) M.-D. Su, S.-Y. Chu, *J. Phys. Chem.* **1997**, 101, 6798; d) M.-D. Su, S.-Y. Chu, *J. Am. Chem. Soc.* **1997**, 119, 10178; e) M.-D. Su, S.-Y. Chu, Chem. *Phys. Lett.* **1998**, 282, 25; f) M.-D. Su, S.-Y. Chu, *Inorg. Chem.* **1998**, 37, 3400.

[5] P. Hoffmann, M. Padmanabhan, *Organometallics* **1983**, 2, 1273.

[6] a) For a discussion, see: W. L. Jorgensen, L. Salem, *The Organic Chemist's Book of Orbitals*, Academic Press, New York, **1973**; b) C. Meredith, T. P. Hamilton, H. F. Schaefer, III, *J. Phys. Chem.* **1992**, 96, 9250.

[7] a) R. D. Bach, J. L. Andres, M.-D. Su, J. J. W. McDouall, *J. Am. Chem. Soc.* **1993**, 115, 5768; b) R. D. Bach, M.-D. Su, E. Aldabagh, J. L. Andres, H. B. Schlegel, *J. Am. Chem. Soc.* **1993**, 115, 10237; c) R. D. Bach, M.-D. Su, *J. Am. Chem. Soc.* **1994**, 116, 10103.

[8] The fully optimized geometries of [CpIr(PH_3)] and [CpRh(PH_3)] at the B3LYP/LANL2DZ level can be found in ref. [4a].

[9] a) M.-D. Su, *Chem. Phys. Lett.* **1995**, 237, 317; b) M.-D. Su, *Chem. Phys.* **1996**, 205, 277; c) M.-D. Su, *J. Phys. Chem.* **1996**, 100, 4339; d) M.-D. Su, *J. Org. Chem.* **1996**, 60, 6621; e) M.-D. Su, *J. Org. Chem.* **1996**, 61, 3080; f) M.-D. Su, *Tetrahedron* **1995**, 51, 12109; g) M.-D. Su, *Tetrahedron* **1995**, 51, 5871.

[10] a) A. H. Janowicz, R. G. Bergman, *J. Am. Chem. Soc.*, **1983**, 105, 3929; b) R. G. Bergman, *Science* **1984**, 223, 902.

[11] W. D. Jones, F. J. Feher, *J. Am. Chem. Soc.* **1984**, 106, 1650.

[12] However, Periana and Bergman (ref. [2b]) suggested that, in contrast to our results, insertion occurs initially into all the C–H bonds of the alkane, but that then even at very low temperatures the secondary insertion products rearrange quickly, and intramolecularly, to the primary products.

[13] a) S. Shaik, H. B. Schlegel, S. Wolfe, *Theoretical Aspects of Physical Organic Chemistry*, Wiley, New York, USA, **1992**; b) A. Pross, *Theoretical and Physical principles of Organic Reactivity*, Wiley, New York, USA, **1995**.

[14] M.-D. Su, *Inorg. Chem.* **1995**, 34, 3829.

[15] R. Hoffmann, *Angew. Chem.* **1982**, *94*, 725; *Angew. Chem. Int. Ed. Engl.* **1982**, 21, 711.

[16] P. E. M. Siegbahn, *J. Am. Chem. Soc.* **1996**, 118, 1487.

[17] a) The $\Delta E_{\sigma\sigma^*}$ was used, in which the triplet state was calculated at B3LYP/LANL2DZ with the singlet geometry of the same level. Also see Methods of Calculation. b) It has to be emphasized that the calculated DFT barrier heights are often, if anything, too low, see: *Chemical Applications of Density Functional Theory* (Eds.: A. Laird, R. B. Ross, T. Ziegler), American Chemical Society, Washington, **1996**. Thus, these barrier values might be underestimated by as much as several kilocalories per mole. It is believed that using the more sophisticated theory with larger basis sets should be essential. Nevertheless, the energies obtained at the B3LYP/LANL2DZ level can, at least, provide reliably qualitative conclusions.

[18] D. F. McMillen, D. M. Golden, *Ann. Rev. Phys. Chem.* **1982**, 33, 493.

[19] A. L. Castelhano, D. Griller, *J. Am. Chem. Soc.* **1982**, 104, 3655.

[20] P. W. Seakins, M. J. Pilling, J. T. Niiranen, D. Gutman, L. N. Krasnoperov, *J. Phys. Chem.* **1992**, 96, 9847.

[21] See an excellent review: P. E. M. Siegbahn, M. R. A. Blomberg, *Theoretical Aspects of Homogeneous Catalysis* (Eds.: P. W. N. M. van Leeuwen, K. Morokuma, J. H. van Lenthe), Kluwer Academic Publishers, Dordrecht, **1995**, and references therein.

[22] R. C. Petry, *J. Am. Chem. Soc.* **1967**, 89, 4600.

[23] a) J. J. Russell, S. M. Senkan, J. A. Seetula, D. Gutman, *J. Phys. Chem.* **1989**, 93, 5184; b) K. M. Ervin, S. Gronert, S. E. Barlow, M. K. Gilles, A. G. Harrison, V. M. Bierbaum, C. H. DePuy, W. C. Lineberger, G. B. Ellison, *J. Am. Chem. Soc.* **1990**, 112, 5750.

[24] D. P. Baldwin, M. A. Buntine, D. W. Chandler, *J. Chem. Phys.* **1990**, 93, 6578.

[25] W. D. Jones, F. J. Feher, *J. Am. Chem. Soc.* **1984**, 106, 1650.

[26] See: ref. [13a], p. 17.

[27] R. A. Marcus, *Annu. Rev. Phys. Chem.* **1964**, 15 and 155, and references therein.

[28] a) A. D. Becke, *Phys. Rev. A* **1988**, 38, 3098; b) C. Lee, W. Yang, R. G. Parr, *Phys. Rev. B* **1988**, 37, 785; c) A. D. Becke, *J. Chem. Phys.* **1993**, 98, 5648.

[29] A. Ricca, C. W. Bauschlicher, *Theor. Chim. Acta.* **1995**, 92, 123.

[30] J. P. Hay, W. R. Wadt, *J. Chem. Phys.* **1985**, 82, 299.

[31] J. P. Hay, W. R. Wadt, *J. Chem. Phys.* **1985**, 82, 284.

[32] Gaussian 94, Revision B.2: M. J. Frisch, G. W. Trucks, H. B. Schlegel, P. M. W. Gill, B. G. Johnson, M. A. Robb, J. R. Cheeseman, T. Keith, G. A. Peterson, J. A. Montgomery, K. Raghavachari, M. A. Al-Laham, V. G. Zakrzewski, J. V. Ortiz, J. B. Foresman, J. Cioslowski, B. B. Stefanov, A. Nanayakara, M. Challacombe, C. Y. Peng, P. Y. Ayala, W. Chen, M. W. Wong, J. L. Andres, E. S. Replogle, R. Gomperts, R. L. Martin, D. J. Fox, J. S. Binkley, D. J. Defrees, J. Baker, J. P. Stewart, M. Head-Gordon, C. Gonzalez, J. A. Pople, Gaussian Inc., Pittsburgh PA, **1995**.

[33] T. H. Dunning, P. J. Hay, *Modern Theoretical Chemistry* (Ed.: H. F. Schaefer), Plenum, New York, **1976**, pp. 1–28.

Received: May 19, 1998 [F1166]